Experimental and Theoretical Investigation of the Molecular and Electronic Structure of $[Zn_4(\mu_4\text{-}S)\{\mu\text{-}S_2As(CH_3)_2\}_6]$ and $[Cd_4(\mu_4\text{-}S)\{\mu\text{-}S_2As(CH_3)_2\}_6]$: Two Possible Molecular Models of Extended Metal Chalcogenide Semiconductors†

Alberto Albinati,‡ Maurizio Casarin,*,§ Chiara Maccato,§ Luciano Pandolfo,§ and Andrea Vittadini⊥

Istituto di Chimica Farmaceutica e Tossicologica, Università di Milano, Milano, Italy; Dipartimento di Chimica Inorganica, Metallorganica ed Analitica, Università di Padova, Padova, Italy; Centro di Studio della Stabilità e Reattività dei Composti di Coordinazione-CNR, Padova, Italy

Received July 31, 1998

The molecular and electronic structure of hexakis[μ-(dimethylarsinodithioate-*S*:*S*′)]-μ_4-thioxotetrazinc has been investigated by combining X-ray diffraction measurements, electrospray mass spectrometry (ESI), UV absorption spectroscopy, and density functional calculations. The polynuclear zinc complex consists of discrete "tetrazinc sulfide" moieties held together by van der Waals interactions. The unit cell contains four independent molecules and four solvent molecules. Each independent unit is characterized by a central μ_4-S coordinated to four Zn ions, each of them at the center of an irregular tetrahedron of S atoms. ESI measurements point out that the synthesis of the analogous Cd derivative was successful. Crystal data are as follows: chemical formula, $C_{12}H_{36}As_6Cl_{1.5}S_{13}Zn_4$; monoclinic space group $P2_1/n$ (no. 14); $a = 30.4228(7)$ Å, $b = 18.3720(5)$ Å, $c = 32.3758(8)$ Å, $\beta = 95.857(1)°$; $Z = 16$. Theoretical calculations indicate that, despite their structural arrangement, neither the Zn nor the Cd complex can be considered molecular models of the extended ZnS and CdS. Nevertheless, the electronic transitions localized in the $Zn_4(\mu_4\text{-}S)$ and $Cd_4(\mu_4\text{-}S)$ inner cores of the title compounds have the same nature as those giving rise to the maxima in the excitation spectra of the extended $Zn_4S(BO_2)_6$ and $Cd_4S(AlO_2)_6$ [Blasse, G.; Dirksen, G. J.; Brenchley, M. E.; Weller, M. T. *Chem. Phys. Lett.* **1995**, *234*, 177].

1. Introduction

A molecular model of a solid is an existing molecule or ion having a local structural arrangement similar to that of the solid and frontier orbitals reproducing the states close to the band gap of the extended material. Molecular models of solids are useful for the insight they directly provide about solid properties and the opportunity of testing—also from an experimental point of view—the validity of the cluster approach[1] to study localized phenomena in extended systems. Some of us have extensively used in the near past the cluster approach joined to the density functional theory (DFT) to investigate local effects in the solid state.[2] In particular, two small polynuclear clusters ($[Zn_4(\mu_4\text{-}O)\{\mu\text{-}O_2CR\}_6]$, R = CH_3,[2a] and $N(C_2H_5)_2$[2b]), both of them characterized by a central μ_4-O tetrahedrally coordinated to four Zn ions, each of them placed at the center of an irregular tetrahedron of O atoms, were shown to be well-tailored molecular models of the bulk ZnO and $Zn_4O(BO_2)_6$. This prompted us to try the synthesis of an analogous thio-derivative ($[Zn_4(\mu_4\text{-}S)\{\mu\text{-}S_2CR\}_6]$), a possible molecular model of bulk ZnS, but any attempt was unsuccessful.

A few years ago, Türk *et al.*[3] proposed as molecular models of CdS a series of Cd thiophenolate-capped clusters of different size ($[Cd(SPh)_4]^{2-}$, $[Cd_4(\mu\text{-}SPh)_6(SPh)_4]^{2-}$, and $[Cd_{10}(\mu_3\text{-}S)_4(\mu\text{-}SPh)_{12}(SPh)_4]^{4-}$, Ph = phenyl). Very recently, Bertoncello *et al.*[4] investigated the electronic structure of a series of zinc thiophenolate-capped ionic/neutral clusters ($[Zn(SPh)_4]^{2-}$, $[Zn_4(\mu\text{-}SPh)_6(SPh)_4]^{2-}$, $Zn_{10}(\mu_3\text{-}S)_4(\mu\text{-}SPh)_{12}$, and $[Zn_{10}(\mu_3\text{-}S)_4(\mu\text{-}SPh)_{12}(SPh)_4]^{4-}$) by combining UV electronic, X-ray photoelectron spectroscopy, and DF calculations. Their results can be summarized as follows: (i) the lowest energy absorption band of Zn clusters always has an intraligand character rather than a ligand to metal charge-transfer (LMCT) nature; (ii) the UV absorption spectra of the Zn clusters are very similar to those of the Cd analogues; (iii) none of the investigated clusters can be considered a molecular model of the bulk ZnS, while the neutral $Zn_{10}(\mu_3\text{-}S)_4(\mu\text{-}SPh)_{12}$ complex was found to be a good molecular model of nonpolar ZnS surfaces. Bertoncello *et al.*[4] also concluded that identical cluster skeletons do not necessarily imply equivalent cluster electronic properties, and great care is needed before claiming that a cluster can be considered as a model of an extended system.

In the late 1972, Johnstone *et al.*[5] reported a brief note about the synthesis and the X-ray structure of a polymetallic zinc complex (hexakis[μ-(dimethylarsinodithioate-*S*:*S*′)]-μ_4-thioxotetrazinc $[Zn_4(\mu_4\text{-}S)\{\mu\text{-}S_2As(CH_3)_2\}_6]$, hereafter **1**). Crystal data,

† In memory of Professor Gastone Paiaro, b. on 9-24-1928, d. on 5-14-1998.

* To whom correspondence should be addressed. Phone 39-049-8275164; fax 39-49-8275161; e-mail casarin@chim01.unipd.it.

‡ Istituto di Chimica Farmaceutica e Tossicologica, Università di Milano.

§ Dipartimento CIMA, Università di Padova.

⊥ CSRCC, CNR di Padova.

(1) Messmer, R. P. *Top. Curr. Phys.* **1977**, *8*, 215.

(2) (a) Bertoncello, R.; Bettinelli, M.; Casarin, M.; Gulino, A.; Tondello, E.; Vittadini, A. *Inorg. Chem.* **1992**, *31*, 1558. (b) Casarin, M.; Tondello, E.; Calderazzo, F.; Vittadini, A.; Bettinelli, M.; Gulino, A. *J. Chem. Soc., Faraday Trans.* **1993**, *89*, 4363.

(3) Turk, T.; Resch, U.; Fox, M. A.; Vogler, A. *J. Chem. Phys.* **1992**, *96*, 3818.

(4) Bertoncello, R.; Bettinelli, M.; Casarin, M.; Maccato, C.; Pandolfo, L.; Vittadini, A. *Inorg. Chem.* **1997**, *36*, 4707.

(5) Johnstone, D.; Fergusson, J. E.; Robinson, W. T. *Bull. Chem. Soc. Jpn.* **1972**, *45*, 3721.

10.1021/ic980914a CCC: $18.00
Published on Web 02/20/1999

though limited to cell parameters, indicated that **1** is characterized by a 3-fold axis and by the presence of an inner core constituted by a μ_4-S atom (hereafter S_C) coordinated to four Zn ions, each of them placed at the center of an irregular tetrahedron of peripheral S atoms (hereafter S_P). More recently, Harrison *et al.*[6] reported the crystal and molecular structure of a similar polymetallic zinc complex ($[Zn_4(\mu_4\text{-}S)\{\mu\text{-}S_2P(OC_2H_5)_2\}_6]$), a byproduct of the synthesis of $[Zn\{S_2P(OC_2H_5)_2\}_2]$.

The presence of the $Zn_4(\mu_4\text{-}S)$ inner core in a molecular compound is in our opinion interesting for at least two reasons: (i) in a recent paper Blasse *et al.*[7] reported and discussed the emission and excitation spectra of $Cd_4(\mu_4\text{-}S)^{6+}$ and $Zn_4(\mu_4\text{-}S)^{6+}$ clusters encapsulated in an aluminate and borate cage, respectively,[8] indicating that the maximum of the charge-transfer optical transition lies at 290 nm (4.28 eV) in the former case and at ~230 nm (5.39 eV) in the latter; (ii) $Zn_4S(BO_2)_6$ and $Zn_4O(BO_2)_6$ are isomorphous, and it has been shown that the spectral properties of $Zn_4O(BO_2)_6$ are very similar to those of $[Zn_4(\mu_4\text{-}O)\{\mu\text{-}O_2CCH_3\}_6]$.[9,10] If we keep in mind that both the cubic ZnS and $Zn_4S(BO_2)_6$ structures include the same $Zn_4(\mu_4\text{-}S)$ unit, we consider interesting a comparison of the spectral properties of **1** with those of ZnS and $Zn_4S(BO_2)_6$. In this regard, it deserves to be mentioned that Trave *et al.*[11] have recently carried out a DF study of $Cd_4(\mu_4\text{-}S)^{6+}$ clusters inside aluminate cages. These authors computed an energy difference between the highest occupied molecular orbital (HOMO) and the lowest unoccupied MO (LUMO) of 2.55 eV, pointing out that both the HOMO and LUMO were most localized on the oxygen atoms of the framework with small contributions from the cluster S atoms.

A further reason for interest in the electronic structure of **1** is the very sharp feature at 351 nm (3.53 eV) in the UV absorption spectrum of the thiophenolate-capped cluster $[Cd_{20}(\mu_4\text{-}S)(\mu_3\text{-}S)_{12}(\mu\text{-}SPh)_{18}(SPh)_4]^{8-}$.[12] Herron *et al.*[12] assigned this narrow band to a transition involving the excitation of an electron from the 3p-based atomic orbitals (AOs) of the central μ_4-S atom to the 5s AOs of the four nearest and 12 next-nearest Cd ions. The synthesis of the Cd analogue of **1** ($[Cd_4(\mu_4\text{-}S)\{\mu\text{-}S_2As(CH_3)_2\}_6]$, hereafter **2**) would then be particularly important not only to compare its electronic properties with those of the bulk CdS and $Cd_4S(AlO_2)_6$ but also to verify the nature of the excitonic feature present in the UV absorption spectrum of $[Cd_{20}(\mu_4\text{-}S)(\mu_3\text{-}S)_{12}(\mu\text{-}SPh)_{18}(SPh)_4]^{8-}$.

In this contribution we report an experimental and theoretical investigation of the molecular and electronic structure of **1** as well as the synthesis and the characterization of the novel Cd complex **2**. The goals of this work are (i) to study the electronic properties of title compounds and (ii) to verify the possibility, suggested by their structure, that they can be considered molecular models of extended systems.

2. Experimental and Computational Details

2.1. Instrumentation, Materials, and Syntheses. All reactions and manipulations were carried out under an atmosphere of dry argon with standard Schlenk techniques. Solvents were distilled under argon before use. H_2S, cacodylic acid ($(CH_3)_2AsO_2H$), and $Zn(ClO_4)_2\cdot 6H_2O$ were purchased from Aldrich, $Cd(NO_3)_2\cdot 4H_2O$ was from Acros, and all were used without further purification. A Siemens SMART diffractometer, cooled by a nitrogen gas stream L.T. device to 198(2) K, was employed for the structural study. UV absorption spectra were recorded on a Varian Cary 5E spectrophotometer. GC/MS determinations were carried out on a FISONS GC 8000 MD 800 instrument, equipped with a capillary column EC-Wax, 30 m, 0.25 mm, 0.25 m, temperature from 50 to 250 °C, 10 °C/min. Electrospray ionization (ESI) mass spectra were collected on a LCQ (Finnigan MAT) instrument, using dilute CH_3OH solutions of the title compounds. Elemental analyses were provided by the Microanalysis Laboratory of the Inorganic Chemistry Department of the University of Padova.

2.2.1. Synthesis of $[(CH_3)_2As(S)\text{-}S\text{-}As(CH_3)_2]$, L. "Cacodyl disulfide", dimethylarsino dimethyldithioarsinate, was prepared according to the procedure described by Bunsen[13] with some modification. Cacodyl acid (3.8 g, 27.5 mmol) was dissolved in 40 mL of C_2H_5OH and 3 mL of H_2O. The vessel was evacuated and connected with a reservoir of H_2S, and the solution was stirred for 1 h, obtaining the formation of a white-cream precipitate. To the suspension was added 50 mL of a 1:1 C_2H_5OH/H_2O solution, obtaining, by stirring, a partial dissolution of the precipitate. The remaining yellow solid (sulfur) was filtered, washed with H_2O and C_2H_5OH, and dried under vacuum. Yield: 0.300 g. The solution was concentrated at 30 °C under vacuum until a white solid formed. The solid was dissolved with the minimum amount of C_2H_5OH, and the solution was left overnight at −10 °C, obtaining a white crystalline precipitate, which was filtered, washed with a cold 1:1 C_2H_5OH/H_2O solution, and then dried under vacuum. Yield of **L**: 2.63 g (19.2 mmol), 70%.

L: mp 64−66 °C. Anal. Calcd for $C_4H_{12}S_2As_2$: C = 17.53, H = 4.41, S = 23.39. Found: C = 17.67, H = 4.24, S = 24.34.

2.2.2. Synthesis of $[Zn_4(\mu_4\text{-}S)\{\mu\text{-}S_2As(CH_3)_2\}_6]$, 1. Compound **1** was synthesized by following the procedure reported by Johnstone *et al.*[5] with some modification. To a solution of **L** (0.463 g, 1.68 mmol) dissolved in 10 mL of C_2H_5OH was added at RT, under stirring, 0.313 g (0.84 mmol) of $Zn(ClO_4)_2\cdot 6H_2O$. After few minutes a white solid formed, and the suspension was then left at −20 °C for 12 h. The microcrystalline solid was filtered off, washed with cold C_2H_5OH, and dried under vacuum. Yield of **1**: 0.130 g (48%), based on Zn. Mother liquors were distilled under vacuum at RT, collecting all volatile compounds in a trap cooled with liquid nitrogen. GC/MS showed the presence of "cacodyle" $[\{(CH_3)_2As\}_2S]$ and other unidentified compounds containing As, S, and O. Compound **1** was recrystallized by slow evaporation of a CH_2Cl_2/*n*-pentane solution, yielding crystals suitable for X-ray analysis.

1: mp > 200 °C. Anal. Calcd for $C_{12}H_{36}S_{13}As_6Zn_4$: C = 11.02, H = 2.77, S = 31.86. Found: C = 11.46, H = 2.62, S = 33.14.

2.2.3. Synthesis of $[Cd_4(\mu_4\text{-}S)\{\mu\text{-}S_2As(CH_3)_2\}_6]$, 2. A solution of 0.2 g of $Cd(NO_3)_2\cdot 4H_2O$ (0.648 mmol) in 10 mL of C_2H_5OH was slowly added, under stirring, to a solution of **L** (0.366 g, 1.335 mmol) in 15 mL of C_2H_5OH. A white solid formed immediately, and the suspension was further stirred for 30 min and then cooled at −20 °C for 5 h. The microcrystalline solid was filtered, washed with 3 mL of cold C_2H_5OH, and dried under vacuum. Yield of **2**: 0.167 g (69%), based on Cd. Mother liquors were distilled as in the case of the Zn derivative, and GC/MS determinations gave the same results.

2: mp > 200 °C. Anal. Calcd for $C_{12}H_{36}S_{13}As_6Cd_4$: C = 9.63, H = 2.42, S = 27.85. Found: C = 10.03, H = 2.30, S = 28.70.

2.3. Structural Study of $1\cdot 0.75(CH_2Cl_2)\cdot 0.25(C_5H_{12})$. A prismatic single crystal of **1** was mounted on a glass fiber at a random orientation on a Siemens SMART diffractometer and cooled by a nitrogen gas stream L.T. device to 198(2) K. The space group was unambiguously determined from the systematic absences, while the cell constants were refined, at the end of the data collection, using 8192 reflections (up to

(6) Harrison, P. G.; Begley, M. J.; Kikabhai, T.; Killer, F. *J. Chem. Soc., Dalton Trans.* **1986**, 925.
(7) Blasse, G.; Dirksen, G. J.; Brenchley, M. E.; Weller, M. T. *Chem. Phys. Lett.* **1995**, *234*, 177.
(8) $Zn_4S(BO_2)_6$ and $Cd_4S(AlO_2)_6$ have a cubic sodalite structure. The boron (aluminum) atom is four-coordinated to oxygen, and these tetrahedra form a three-dimensional network containing cavities. The tetrahedral $Zn_4(\mu_4\text{-}S)^{6+}$ and $Cd_4(\mu_4\text{-}S)^{6+}$ clusters, characterized by a central μ_4-S atom surrounded by four Zn/Cd ions, fit into the cubooctahedral cavities.
(9) (a) Meijerink, A.; Blasse, G.; Glasbeek, M. *J. Phys.: Condens. Matter* **1990**, *2*, 6303. (b) Blasse, G. *Chem. Phys. Lett.* **1990**, *175*, 237.
(10) Kunkely, H.; Vogler, A. *J. Chem. Soc., Chem. Commun.* **1990**, 1204.
(11) Trave, A.; Buda, F.; Selloni, A. *J. Chem. Phys.* **1998**, *102*, 1522.
(12) Herron, N.; Suna, A.; Wang, Y. *J. Chem. Soc., Dalton Trans.* **1992**, 2329.
(13) Bunsen, R. W. *Ann. Chem.* **1843**, *2*, 46.

Table 1. Crystallographic Data for **1**·0.75(CH_2Cl_2)·0.25(C_5H_{12})

chemical formula	$C_{12}H_{36}As_6Cl_{1.5}S_{13}Zn_4$
a, Å	30.4228(7)
b, Å	18.3720(5)
c, Å	32.3758(8)
β, deg	95.857(1)
V, Å^3	18001.3(8)
Z	16
formula weight	1361.51
space group	$P2_1/n$ (no. 14)
T, °C	−75(2) °C
λ, Å	0.710 73
$\rho_{(calcd)}$, g cm^{-3}	2.051
μ, cm^{-1}	7.189
R^a	0.042
$R_w{}^2$ ^{b}	0.1305

^{a} $R = \sum(|F_o - (1/k)F_c|)/\sum|F_o|$. ^{b} $R_w{}^2 = [\sum w(F_o{}^2 - (1/k)F_c{}^2)^2/\sum w|F_o{}^2|^2]$.

$\theta_{max} \leq 49°$) with the Siemens data reduction software XSCAN. The asymmetric unit consists of four independent molecules of **1**.

The data were collected in "ω-scan mode" with steps of 0.3°. For each of the resulting 1271 "frames", counting time was 20 s. Data were corrected for Lorentz and polarization factors; an empirical absorption correction (based on the intensities of symmetry-related reflections) was also applied using the SADABS program.[14]

Selected crystallographic and other relevant data are listed in Table 1 and S1 (Supporting Information). The standard deviations on intensities were calculated in term of statistics alone, while those on $F_o{}^2$ were calculated as shown in Table S1.

The structure was solved by direct and Fourier methods and refined by full-matrix least-squares,[15] minimizing the function $\sum w(F_o{}^2 - (1/k)F_c{}^2)^2$. During the refinement, the Fourier difference maps revealed chlathrated molecules of dichloromethane, which were refined without constraints, and a highly disordered pentane molecule. It proved impossible to model satisfactorily all the pentane orientations; therefore, only the strongest peaks from the Fourier map were retained and refined, even though with the expected large displacement parameters.

Anisotropic displacement parameters were used for all atoms except the pentane carbon atoms, which were refined isotropically. The contribution of the hydrogen atoms, in their calculated position (C−H = 0.95 Å, $B = 1.5 \times B_{(carbon)}$ Å^2), was included in the refinement using a riding model. No extinction correction was deemed necessary. The scattering factors used, corrected for the real and imaginary parts of the anomalous dispersion, were taken from the literature.[16] All calculations were carried out by using the PC version of the SHELX-97 programs.[15]

2.4. Absorption Spectra. RT absorption spectra of **1** were recorded in the 200−500 nm region by using a Varian Cary 5E spectrophotometer with a spectral bandwidth of 1 nm. Solutions of 10^{-5}−10^{-6} M, obtained by dissolving **1** in spectral grade CH_2Cl_2, were employed immediately after their preparation. The very low solubility of **2** in whatever solvent did not allow us to obtain acceptable quality UV absorption spectra.

2.5. Theoretical Study of 1 and 2. All the calculations have been run by using the DMol code.[17] This is a DF numerical method where the Kohn−Sham equations are solved for systems with a finite size, providing energy eigenvalues, eigenvectors, and charge distribution and allowing the analytic evaluation of energy gradients (force calculations) by using numeric atomic orbital (NAO) basis sets. The following NAOs have been employed: (a) Cd: the 1s−5s NAOs of the neutral cadmium atom, the 4d−5p NAOs of Cd^{2+}; (b) As: the 1s−4p NAOs of the neutral arsenic atom, the 3d−4d NAOs of As^{2+}; (c) Zn: the 1s−4s NAOs of the neutral zinc atom, the 3d−4p NAOs of Zn^{2+}; (d) S: the 1s−3p NAOs of the neutral sulfur atom, the 3s−3d NAOs of S^{2+}; (e) C: the 1s−2p NAOs of the neutral carbon atom, the 2s−2p NAOs of C^{2+} and two sets of 1s, 2p, and 3d NAOs generated from two hydrogenic calculations using $Z = 5$ and $Z = 7$; (f) H: the 1s NAO of the neutral hydrogen atom and two sets of 1s and 2p NAOs generated from two hydrogenic calculations using $Z = 1.3$ and $Z = 4$. The Cd 1s−3d, the As/Zn 1s−2p, and the S/C 1s NAOs have been kept frozen throughout the calculations in a fully occupied configuration, allowing their exclusion from the variational space. As far as the *l* value of the one-center expansion of the Coulomb potential about each nucleus is concerned, a value of *l* one greater than that in the atomic basis set has been found to provide sufficient precision. The following degree of angular truncation has been used throughout the calculations: $l = 3$ for Cd, Zn and $l = 2$ for As, S, C, H.

Finally, instead of displaying discrete eigenvalues along an energy axis, we preferred to plot the density of states (hereafter DOS) as a function of energy by using a 0.3 eV Lorentzian broadening factor. These plots, based on the Mulliken's prescription for partitioning the overlap density,[18] have the advantage of providing insights into the atomic composition of MOs over a broad range of energy. The Mulliken population analysis,[18] even though uniquely defined, is rather arbitrary; nevertheless, it is very useful to gain at least a qualitative idea of the electron localization. Selected MO plots have also been reported to assign the character of particular MOs. All the calculations have been performed on an IBM 6000/550 workstation at the Inorganic Chemistry Department of the University of Padova.

3. Results and Discussion

We already pointed out that, in the attempt of determining the reaction stoichiometry of the synthesis of **1** and **2**, we have distilled the reaction mother liquors, collecting all volatile compounds in a liquid nitrogen trap. The condensed vapors were examined by GC/MS, and in both cases, we observed the same signals in the chromatograms. Unfortunately, we were able to identify only cacodyle, [{$(CH_3)_2As$}$_2$S], while the other signals corresponded to unidentified compounds containing As, S, and O. These compounds can be formed in the reactions, but they could even be produced by thermal decomposition during GC/MS determinations or by collateral reactions with the solvent and/or with the strong oxidizing anions (NO_3^- and ClO_4^-). On this basis, we are unable to propose any stoichiometry for the synthesis of **1** and **2**, and we can only report that the highest reaction yields are obtained with reaction ratios **L**/metal = 2.

3.1. Crystal Structure of 1·0.75(CH_2Cl_2)·0.25(C_5H_{12}). The structure of **1** consists of discrete "tetrazinc sulfide" moieties held together by van der Waals interactions. There are four independent molecules in the unit cell and four chlathrated solvent molecules (dichloromethane and pentane in a 3:1 ratio). The unit cell constants are the same as those already reported, for one of the crystal forms of the same complex, by Johnston *et al*.[5] The geometries of the four independent units are very similar with only small differences in the bond lengths and bond angles, which may be explained by the conformational nonrigidity of the ligands. Moreover, the trends shown by the values of the bond distances and angles are the same for each of the four independent molecules, and in the forthcoming discussion, we will use the geometry of just one molecule. An ORTEP view of compound **1** is given in Figure 1a, while a selection of distances and angles are listed in Table 2. The full numbering scheme of all molecules and an extended list of bond distances and bond and torsion angles are given in the Supporting Information.

The molecule consists of a central S atom tetrahedrally coordinated to four Zn atoms bound to six dithiodimethylarseniate(V) ([S−As$(CH_3)_2$−S]$^-$) ligands. The coordination around

(14) Sheldrick, G. M. *SADABS*; Universität of Göttingen.
(15) Sheldrick, G. M. *SHELX-97*, Structure solution and refinement package; Universität of Göttingen, 1993.
(16) *International Tables for X-ray Crystallography*; Wilson, A. J. C., Ed.; Kluwer Academic Publisher: Dordrecht, The Netherlands, 1992; Vol. C, Tables 6.1.1.4, 4.2.6.8, 4.2.4.2.
(17) *Dmol 2.2*; Biosym Technologies, San Diego, CA, 1992.
(18) Mulliken, R. S. *J. Chem. Phys.* **1955**, *23*, 1833.

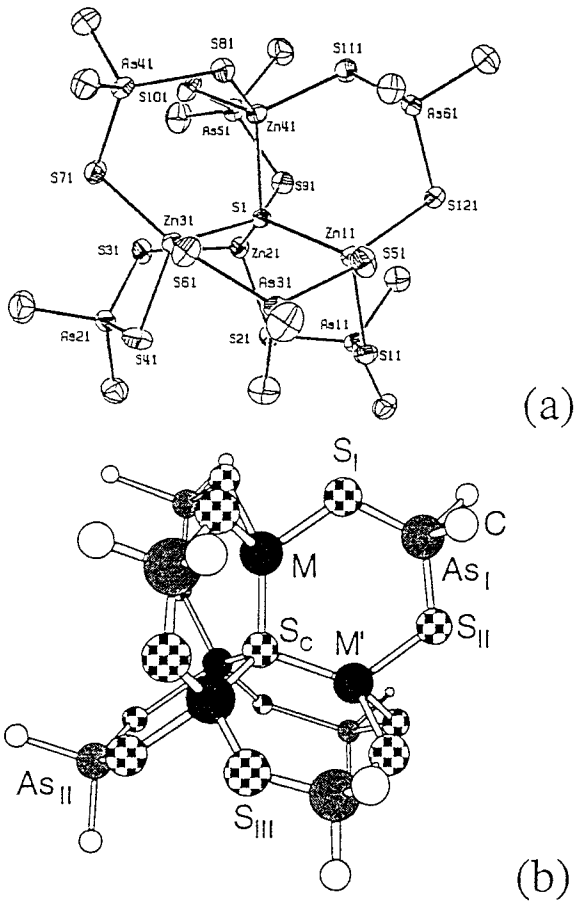

Figure 1. (a) ORTEP plot of one of the four independent molecules (see text) of **1**, with the atom-numbering scheme; (b) schematic representation of the idealized (C_{3v}) structure of $[M_4(\mu_4\text{-}S)\{\mu\text{-}S_2As(CH_3)_2\}_6]$ adopted for theoretical calculations. Hydrogen atoms are not included for the sake of clarity.

Table 2. Selected List of Experimental Bond Lengths (Å) and Angles (deg) for Compound **1**[a]

S1−Zn11	2.321(2)	Zn11−S1−Zn31	114.71(9)
S1−Zn21	2.334(2)	Zn11−S1−Zn21	114.98(9)
S1−Zn31	2.329(2)	Zn21−S1−Zn31	104.45(8)
S1−Zn41	2.341(2)	Zn11−S1−Zn41	115.31(9)
Zn11−S121	2.353(2)	Zn21−S1−Zn41	103.63(8)
Zn11−S11	2.351(2)	Zn31−S1−Zn41	102.17(8)
Zn11−S51	2.351(2)	As−S−Zn[b]	104.8 ± 9
Zn21−S21	2.347(2)	S−As−S[b]	117.3 ± 1.0
Zn21−S31	2.333(2)		
Zn21−S91	2.371(2)		
Zn31−S61	2.353(2)		
Zn31−S41	2.352(2)		
Zn31−S71	2.336(2)		
Zn41−S101	2.334(2)		
Zn41−S81	2.345(2)		
Zn41−S111	2.339(2)		
As1−S1[b]	2.140 ± 5		

[a] The values listed refer to one of the four independent molecules in the unit cell (see text); esd's are given in parentheses. [b] Average value, the ± sign refers to the esd of the mean.

the S atom shows a tetragonal distortion, resulting in two short and two long Zn−S separations (av 2.325(2) and 2.337(2) Å, respectively). The individual Zn−S separations are normal[19] and span the interval 2.37−2.32 Å (av 2.337(13) Å). The As−S and As−C distances (av 2.139(5) and 1.921(9) Å, respectively) are unexceptional and, again, fall in the expected range.[19] The above-mentioned pattern is also present in the values of the Zn−S−Zn and S−Zn−S angles (av 112.5(2)° and 106.3(2)°, respectively) and may be induced by the different conformations of the six-member rings formed by the Zn, S, and As atoms. The outer angles (i.e., Zn−S−As and S−As−S, involving the As atoms of the ligands) have average values of 105° and 117°, respectively. As also found by Johnstone *et al.*,[5] three of these rings are in a slightly distorted chair conformation, while the other three are in a twist-boat arrangement. Each "tetrazinc sulfide" moiety, as required by the molecular symmetry, is chiral, and therefore the crystal is a racemate.

3.2. Electrospray Ionization (ESI) Mass Spectrometry of 1 and 2. The gas-phase behavior of compounds **1** and **2** has been examined by ESI mass spectrometry. This technique, the application of which to the organometallic chemistry has been recently reviewed and discussed,[20] was very useful to study compounds **1** and **2**. As a matter of fact, even with a "soft" desorption and ionization method such as fast atom bombardment, we were unable to obtain reliable information on the molecular weight and the structure of the title compounds because of their extended fragmentation (only signals at relatively low *m*/*z* values were observed). At variance with that, clear signals corresponding to molecular ions for **1** and **2** were measured by means of ESI mass spectrometry. Measurements have been performed on 10^{-5} (10^{-7}) M solutions of **1** (**2**) in CH_3OH. The lower concentration of the CH_3OH solution of **2** is due to its lower solubility.

The ESI spectra of **1** and **2** are reported in Figure 2 together with the relative simulated isotopic clusters. The inspection of the figure clearly indicates in **1** the presence of a signal centered at *m*/*z* 1330, corresponding to $[\mathbf{1} + Na]^+$. As far as **2** is concerned, it is possible to observe, despite the great noise/signal ratio (a consequence of the low solubility of **2**), a signal centered at *m*/*z* 1552, corresponding to $[\mathbf{2} + CH_3OH + Na]^+$. The correspondence between experimental data and the simulated isotopic clusters is definitely good. Moreover, ms/ms experiments show the same primary loss (a $S-As(CH_3)_2-S$ fragment) for the ions at *m*/*z* 1330 (**1**) and 1552 (**2**), making us quite confident that **2** has the same structure as **1**.

3.3. Absorption Spectroscopy Measurements. The spectral pattern of **1** between 230 and 350 nm, measured immediately after its dissolution in spectral grade CH_2Cl_2, is shown in Figure 3. Besides the absence of any sharp spectral feature at $\lambda > 300$ nm, the spectrum consists of an evident shoulder at 277 nm (4.48 eV), a well-defined band at 248 nm (5.00 eV), and a strong absorption, the edge of which lies at 240 nm (5.17 eV, the corresponding maximum has not been detected because at $\lambda <$ 230 nm the solvent starts to interfere). Interestingly, the energy position of this last band agrees very well with results reported by Blasse *et al.*[7] about the absorption maximum in the excitation spectrum of $Zn_4(\mu_4\text{-}S)^{6+}$ clusters encapsulated in a borate cage.

The spectral pattern of **2** in CH_2Cl_2 is not reported because of its poor quality. Nevertheless, it has to be emphasized that no sharp feature for 300 nm $< \lambda <$ 400 nm was observed.

3.4. Theoretical Results. The low solubility of **2** prevented us from obtaining crystals suitable for an X-ray study. Nevertheless, elemental analysis data and ESI mass spectrometry results collected for **2** are consistent with a molecular structure analogous to that of **1**. Numerical experiments pertaining to **2** have been carried out within this assumption.

(19) Orpen, A. G.; Brammer, L.; Allen, F. H.; Kennard, O.; Watson, D. G.; Taylor, R. *J. Chem. Soc., Dalton Trans.* **1989**, S1.

(20) Colton, R.; D'Agostino, A.; Traeger, J. C. *Mass Spectrosc. Rev.* **1995**, *14*, 79.

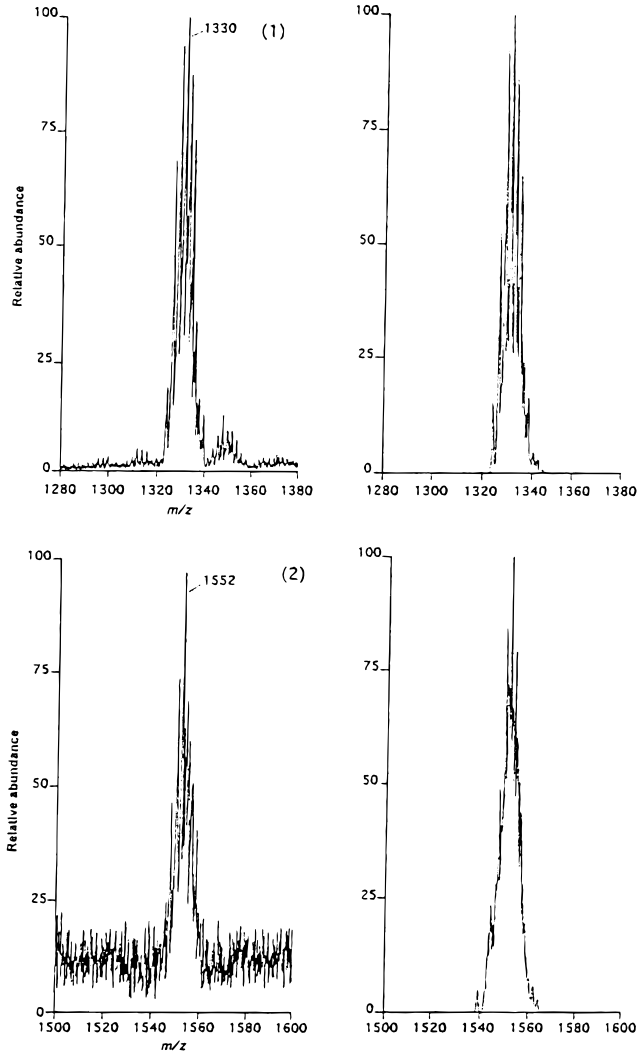

Figure 2. Electrospray mass spectrometry of **1** and **2**. Simulated isotopic clusters are also displayed.

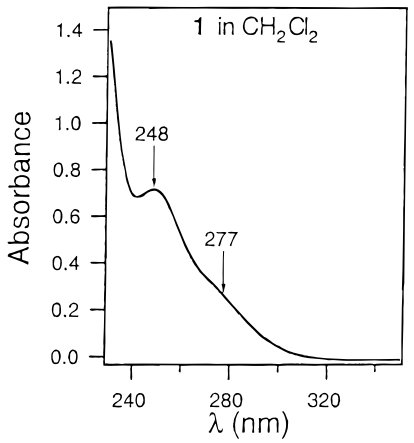

Figure 3. UV absorption spectra of $[Zn_4(\mu_4\text{-}S)\{\mu\text{-}S_2As(CH_3)_2\}_6]$ in CH_2Cl_2.

The coordinates of all the 71 atoms of **1** and **2** have been optimized by assuming a C_{3v} symmetry for both clusters. Such a constraint is not so severe for the isolated molecules because crystallographic data (see above) are consistent with a conformational nonrigidity of the $S_C-M-S_P-As-S_P-M'$ rings (see Figure 1b). In Table 3 the optimized geometrical parameters of **1** and **2** are reported. Theoretical bond lengths and bond angles of the $Zn_4(\mu_4\text{-}S)$ inner core agree well with crystallographic measurements (see Table 2). In contrast to that, a poorer agreement is found for structural parameters (in particular bond angles) of the $[S-As(CH_3)_2-S]$ fragments (a consequence of the idealized C_{3v} structure we assumed in our calculations). The analysis of Table 3 also points out that the structural parameters most affected on passing from **1** to **2** are the S_C-M and S_P-M bond lengths, an effect of the larger Cd^{2+} ionic radius (0.92 Å) compared to that of the Zn^{2+} ion (0.69 Å).[21]

Table 3. Selection of Optimized Bond Lengths (Å) and Bond Angles (deg) of $[Zn_4(\mu_4\text{-}S)\{\mu\text{-}S_2As(CH_3)_2\}_6]$ (**1**) and $[Cd_4(\mu_4\text{-}S)\{\mu\text{-}S_2As(CH_3)_2\}_6]$ (**2**) in Parentheses[a-c]

S_C-M	2.32(2.49)	$M'-S_C-M$	109(110)
S_C-M'	2.32(2.47)	$M'-S_C-M'$	110(109)
S_I-M	2.34(2.53)	S_C-M-S_I	125(124)
$S_{II}-M'$	2.33(2.54)	S_I-M-S_I	90(92)
$S_{III}-M'$	2.35(2.53)	$M-S_I-As_I$	118(117)
S_I-As_I	2.13(2.14)	$S_I-As_I-S_{II}$	123(128)
$S_{II}-As_I$	2.14(2.14)	$M'-S_{II}-As_I$	119(121)
$S_{III}-As_{II}$	2.13(2.14)	$S_C-M'-S_{II}$	125(121)
$C-As_I$	1.92(1.92)	$S_{II}-M'-S_{III}$	91(93)
$C-As_{II}$	1.92(1.92)	$S_{III}-M'-S_{III}$	91(94)
$C-H^d$	1.10(1.10)	$S_C-M'-S_{III}$	125(124)
		$M'-S_{III}-As_{II}$	119(118)
		$S_{III}-As_{II}-S_{III}$	123(128)

[a] Atoms have been labeled according to Figure 1b, rather than as in Table 2 and Figure 1a. [b] The optimization procedure has been carried out by assuming an idealized C_{3v} symmetry. [c] Only the unique atoms, with the exclusion of the CH_3 group, have been labeled. [d] Mean value.

A qualitative description of the bonding scheme of $[M_4(\mu_4\text{-}S)\{\mu\text{-}S_2As(CH_3)_2\}_6]$ simply based on symmetry arguments and overlap considerations may now be useful. Within the idealized C_{3v} symmetry, the 12 S_P atoms can be divided into three distinct sets: (i) set $\mathbf{S}_I$, composed of the three sulfur atoms directly bound to the axial M atom (S_I in Figure 1b); (ii) set $\mathbf{S}_{II}$, constituted by the three sulfur atoms S_{II} of the $S_CMS_IAsS_{II}M'$ rings containing the 3-fold axis; and (iii) set $\mathbf{S}_{III}$, including the six symmetry-related sulfur atoms S_{III} of the $S_CM'S_{III}AsS_{III}M'$ rings. If we neglect the σ backbone of the $[S-As(CH_3)_2-S]^-$ ligand, its outermost occupied orbitals are (i) the in-phase (n^+) and out-of-phase (n^-) linear combinations of the S_P lone pairs lying in the S_P-As-S_P plane and (ii) the symmetric (π_1) and antisymmetric (π_2) combinations of S_P 3p AOs perpendicular to the S_P-As-S_P planes. Incidentally, we adopted here the same labels usually employed for the valence manifold MOs of carboxylic acids: π_1 and π_2 identify the orbitals O−C−O as totally bonding and nonbonding, respectively.

At variance with the $[O-CR-O]^-$ ligand, where the energy difference between π_1 and π_2 orbitals is quite large (~3 eV in $HCOO^-$)[22] as a consequence of their different O−C−O bonding character, the absence of any π interaction delocalized over $[S-As(CH_3)_2-S]^-$ should give rise to a negligible $\Delta E_\pi = E_{\pi 2} - E_{\pi 1}$. To estimate ΔE_π, the eigenvector spectrum of the free $[S-As(CH_3)_2-S]^-$ anion has been computed by assuming the same optimized bond distances and bond angles of the coordinate ligand. The following energy difference and gross atomic charges (Q) are obtained: $\Delta E_\pi = 0.07$ eV; $Q_{As} = 0.40$, $Q_S = -0.65$, $Q_{CH3} = -0.05$.

The high-energy region of the $[M_4(\mu_4\text{-}S)\{\mu\text{-}S_2As(CH_3)_2\}_6]$ eigenvalue spectrum should include 24 levels reminiscent of the $[S-As(CH_3)_2-S]^-$-based n^+, n^-, π_1, and π_2 MOs somehow mixed with the S_C 3p AOs. The orbitals localized on $\mathbf{S}_I$ and $\mathbf{S}_{II}$

(21) Cotton, F. A.; Wilkinson, G. *Advanced in Inorganic Chemistry*, 5th ed.; Wiley-Interscience: New York, 1988.
(22) Casarin, M.; Maccato, C.; Vittadini, A. *J. Chem. Soc., Faraday Trans.* **1998**, *94*, 797.

Table 4. Atomic Character from DMOL Calculations of Idealized $[Zn_4(\mu_4\text{-}S)\{\mu\text{-}S_2As(CH_3)_2\}_6]$

		population %																
	eigenvalue	S_C			4Zn			$3S_I$			$3S_{II}$			$6S_{III}$				
MO	$-\epsilon$ (eV)	s	p	d	s	p	d	s	p	d	s	p	d	s	p	d	6As	$12CH_3$	character
$57a_1$	1.96	0	0	0	1	0	1	1	15	6	0	5	1	1	19	3	29	18	
81e	1.98	0	0	0	2	2	1	0	7	1	1	12	4	2	19	7	30	12	$a_1 + t_2$
$56a_1$*[a]	2.74*	1	0	0	6	4	1	0	9	3	0	10	3	1	19	7	23	13	
$27a_2$	5.13	0	0	0	0	0	0	0	58	1	0	11	0	0	20	0	8	2	
$26a_2$	5.14	0	0	0	0	0	0	0	27	0	0	18	0	0	40	0	8	7	
80e	5.14	0	0	0	0	0	0	0	0	0	0	23	0	0	55	1	7	14	
$55a_1$	5.69	0	0	0	0	0	2	0	0	0	0	14	0	0	65	0	7	12	$S_P\ 3p_\pi$
79e	5.69	0	0	0	0	0	2	0	26	0	0	22	0	0	31	0	7	12	$(a_2 + e + 2t_1 + t_2)$
78e	5.71	0	0	0	0	1	2	0	7	0	0	23	0	0	55	0	7	5	
$25a_2$	5.71	0	0	0	0	1	2	0	0	0	0	30	0	0	58	0	6	3	
77e	5.72	0	0	0	0	1	2	0	50	0	0	14	0	0	22	0	6	5	
76e	6.12	0	0	0	0	5	0	1	31	0	1	21	0	0	33	0	5	3	
$24a_2$	6.13	0	0	0	0	5	1	0	0	0	0	24	0	2	62	0	5	1	
75e	6.48	0	0	1	2	7	1	0	24	0	0	9	0	1	47	0	5	3	$S_P\ 3p_\sigma$
$54a_1$	6.48	0	1	1	1	7	2	0	7	0	1	40	0	0	30	0	5	5	$(e + t_1 + 2t_2)$
74e	6.54	0	23	0	1	6	5	0	5	0	1	18	0	1	32	0	6	2	$+ S_C\ 3p$
$53a_1$	6.56	0	23	0	1	5	5	2	37	0	1	8	0	0	13	0	5	0	
73e	6.78	0	0	1	0	11	2	0	19	0	0	19	0	0	37	0	7	4	
$52a_1$	8.13	2	0	0	17	1	1	2	16	0	2	15	0	3	31	0	10	0	$S_P\ 3p_\sigma\ (a_1)$
72e	8.37	0	0	0	0	3	6	3	19	1	3	18	1	2	13	1	20	10	
$23a_2$	8.37	0	0	0	0	3	6	0	0	0	0	2	0	7	48	2	20	12	
71e	8.55	0	20	0	2	5	2	1	9	0	0	0	0	3	17	1	18	22	$S_C\ 3p\ (t_2)$
$51a_1$	8.55	0	20	0	1	5	2	0	1	0	3	19	0	1	6	2	18	22	

[a] *Lowest unoccupied MO.

Table 5. Atomic Character from DMol Calculations of Idealized $[Cd_4(\mu_4\text{-}S)\{\mu\text{-}S_2As(CH_3)_2\}_6]$

		population %																
	eigenvalue	S_C			4Cd			$3S_I$			$3S_{II}$			$6S_{III}$				
MO	$-\epsilon$ (eV)	s	p	d	s	p	d	s	p	d	s	p	d	s	p	d	6As	$12CH_3$	character
$57a_1$	2.10	0	0	0	30	2	1	0	5	2	0	2	1	0	28	2	20	7	
81e	2.12	0	0	0	2	3	1	0	6	1	2	11	2	1	27	5	29	10	$a_1 + t_2$
$56a_1$*[a]	2.73	0	0	0	16	7	1	0	8	2	0	9	2	1	21	6	19	8	
$27a_2$	5.35	0	0	0	0	0	0	0	80	1	0	3	0	0	2	0	7	7	
80e	5.40	0	0	0	0	0	0	0	0	0	0	35	0	0	50	0	7	8	
$26a_2$	5.43	0	0	0	0	0	0	0	6	0	0	37	0	0	48	0	7	2	
79e	5.72	0	0	0	0	1	1	0	55	0	0	10	0	0	17	0	7	9	$S_P\ 3p_\pi$
$55a_1$	5.74	0	0	0	0	0	2	0	1	0	0	14	0	0	68	0	6	9	$(a_2 + e + 2t_1 + t_2)$
78e	5.76	0	0	0	0	0	2	0	29	0	0	30	0	0	29	0	6	4	
$25a_2$	5.78	0	0	0	0	0	2	0	0	0	0	31	0	0	57	0	6	4	
77e	5.79	0	0	0	0	0	2	0	2	0	0	20	0	0	66	0	6	6	
76e	6.16	0	0	0	0	6	1	0	33	0	1	25	0	0	27	0	4	3	
$24a_2$	6.21	0	0	0	0	6	1	0	0	0	0	14	0	1	72	0	4	2	
$54a_1$	6.39	0	0	0	2	7	1	0	12	0	1	46	0	0	23	0	5	3	$S_P\ 3p_\sigma$
75e	6.42	0	4	0	1	8	1	0	28	0	0	8	0	0	38	0	6	6	$(e + t_1 + 2t_2)$
74e	6.52	0	19	0	2	5	2	0	3	0	0	16	0	2	44	0	5	2	$+ S_C\ 3p$
$53a_1$	6.56	0	23	0	1	6	4	1	33	0	1	6	0	0	18	0	6	1	
73e	6.67	0	1	1	0	11	2	0	14	0	0	13	0	0	46	0	7	5	
$52a_1$	7.92	1	0	0	20	0	1	1	17	0	1	14	0	2	29	0	9	5	$S_P\ 3p_\sigma\ (a_1)$
72e	8.41	0	36	0	7	7	2	1	14	0	1	5	0	0	7	0	9	11	$3p\ S_C\ (t_2)$
$51a_1$	8.42	0	40	0	7	8	2	1	4	0	1	13	0	0	5	1	9	9	
71e	8.51	0	6	0	1	3	3	2	10	0	2	17	1	3	20	1	19	12	
$23a_2$	8.54	0	0	0	0	2	3	0	0	0	0	1	0	7	51	1	20	15	

[a] *Lowest unoccupied MO.

sets transform as $a_1 + e\ (n^+)$, $a_1 + e\ (n^-)$, $a_2 + e\ (\pi_1)$, $a_2 + e\ (\pi_2)$, while the $\mathbf{S}_{III}$-based ones span the following irreducible representations: $a_1 + e\ (n^+)$, $a_2 + e\ (n^-)$, $a_1 + e\ (\pi_1)$, $a_2 + e\ (\pi_2)$. Elementary overlap considerations suggest that the frontier orbitals most affected by the interaction between the $M_4(\mu_4\text{-}S)^{6+}$ inner core and the $[S{-}As(CH_3)_2{-}S]^-$ ligand should be the formally empty Zn (Cd)-based 4sp (5sp) AOs and the occupied, S_P-based n^+/n^- levels pointing directly toward the M atoms. It is reasonable to expect that the above indicated 24 orbitals will then be factored into two groups: in the outermost energy region the 12 linear combinations $(a_1 + 3a_2 + 4e)$ of the orbitals related to the $[S{-}As(CH_3)_2{-}S]^-$ π_1 and π_2 levels, while, at lower energies, the remaining 12 $(3a_1 + a_2 + 4e)$ MOs deriving from the n^+ and n^- linear combinations, stabilized by the bonding interaction with empty orbitals of the $M_4(\mu_4\text{-}S)^{6+}$ inner core.

In Tables 4 and 5 we have reported the ground-state charge density analysis of the uppermost MOs of **1** and **2**, respectively. In both cases we have included 30 occupied levels (considering their degeneracies) to pick up not only the 24 combinations mainly localized on the $[S{-}As(CH_3)_2{-}S]^-$ ligands (see above) but also some of the MOs having a high localization on the S_C 3p AOs. The inspection of both tables shows that the qualitative picture of the bonding scheme we proposed for **1** and **2** agrees

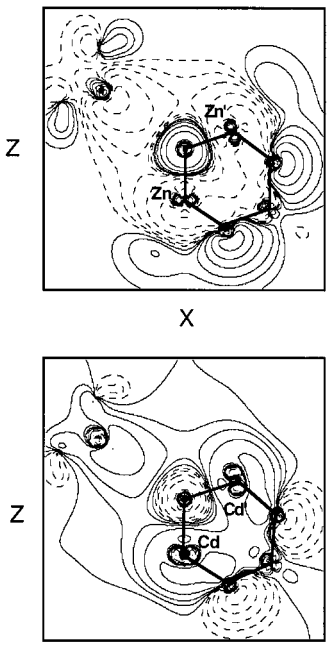

Figure 4. Contour plot of the $52a_1$ MO of **1** (top) and **2** (bottom). Both contour plots lie in the *xz* plane. Contour values are ±0.8, ±0.4, ±0.2, ±0.1, ... $e^{1/2} \times Å^{-3/2}$. Negative values in dashed lines.

very well with DF outcomes. Actually, both in **1** and **2**, the orbitals accounting for the linear combinations of the $[S-As(CH_3)_2-S]^-$ π_1/π_2 levels (the 12 closely spaced MOs from the $27a_2$ HOMO to the 77e MO) are quite well separated from those deriving from the $[S-As(CH_3)_2-S]^-$ n^+ and n^- levels (the 76e−73e MOs). The 12th combination of the in-plane S_P lone pairs (the $52a_1$ MO, see Tables 4 and 5) lies, in both cases, deeper in energy than the remaining n^+/n^- σ MOs and quite close to S_C 3p-based orbitals. The analysis of its bonding character indicates that it accounts for a bonding interaction between the totally symmetric combination of the four Zn 4s (Cd 5s) AOs and a suitable linear combination of the S_P n^+ lone pairs (see Figure 4).

Interestingly, the lowering of symmetry from a structure where the four M and the 12 S_P atoms gives rise to two sets of equivalent species (T_d symmetry) to the one we adopted for the calculations (C_{3v}) has only minor effects on the energy level degeneracies. For this reason the assignment of the UV absorption spectra of **1** (see below) will be based on an ideal tetrahedral environment of the μ_4-S atom. In this regard, it can be useful to note that the M s, p, and d AOs of the $M_4(\mu_4\text{-S})$ inner core give rise, in T_d symmetry, to the following linear combinations: $(a_1 + t_2)$, $(a_1 + e + t_1 + 2t_2)$, and $(a_1 + 2e + 2t_1 + 3t_2)$, respectively. The interaction of 3p S_C AOs (transforming as t_2 in a tetrahedral environment) with empty t_2 orbitals (4s/4p and 5s/5p in **1** and **2**, respectively) gives rise to only occupied bonding combinations, while the interaction with filled t_2 levels (3d and 4d in **1** and **2**, respectively) originates occupied bonding (mainly localized on the metal atoms) and antibonding partners.

In Figure 5 the DOS of **1** and **2** are reported together with the partial DOS (PDOS) of M, S_C, S_P, and As. Among the occupied levels at $E > -10$ eV, the S_C 3p-based AOs give rise to two peaks lying at ∼−9.0 and ∼−6.5 eV in **1** and ∼−8.5 and ∼−6.5 eV in **2**. Peaks at −9.0 and −8.5 eV include MOs having a M−S_C bonding character, while MOs accounting for an antibonding interaction between S_C 3p AOs and Zn 3d (Cd 4d) occupied orbitals are hidden under the peaks at −6.5 eV.

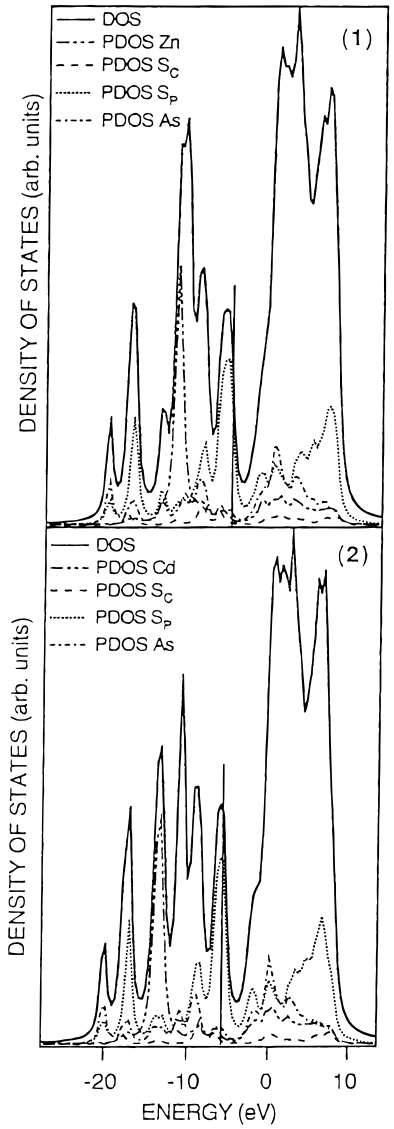

Figure 5. Density of states (DOS) of $[M_4(\mu_4\text{-S})\{\mu\text{-}S_2As(CH_3)_2\}_6]$ (M = Zn and Cd); partial DOS (PDOS) of M, S_C, S_P, and As are also displayed.

Table 6. Effective Atomic Charges from Mulliken Populations Analysis for $[Zn_4(\mu_4\text{-S})\{\mu\text{-}S_2As(CH_3)_2\}_6]$ (**1**) and $[Cd_4(\mu_4\text{-S})\{\mu\text{-}S_2As(CH_3)_2\}_6]$ (**2**)

	1	**2**
S_C	−0.61	−0.79
M	0.52	0.69
M′	0.52	0.69
S_I	−0.38	−0.43
S_{II}	−0.38	−0.43
S_{III}	−0.38	−0.43
As	0.33	0.32

In detail, the $50a_1 + 69e + 51a_1 + 71e$ MOs give rise to the low-energy peak of **1** and **2**, while the high-energy one includes, in both clusters, the $74e + 53a_1$ MOs. It is noteworthy that the $50a_1$ and 69e MOs (not included in Tables 4 and 5) represent the main source of the Zn−S_C σ bonding, while the major contributions to the Cd−S_C direct interaction are provided by the $51a_1$ and 71e MOs.

Q values of selected atoms are reported in Table 6, while in Table 7 selected overlap populations (OP) are collected. Data of Table 6 indicate that (i) Q_{As} is substantially the same in **1** and **2**; (ii) Q_{S_C} is significantly more negative than Q_{S_P} in both

Table 7. Selected Overlap Populations of $[Zn_4(\mu_4\text{-}S)\{\mu\text{-}S_2As(CH_3)_2\}_6]$ (**1**) and $[Cd_4(\mu_4\text{-}S)\{\mu\text{-}S_2As(CH_3)_2\}_6]$ (**2**)

	1				**2**			
	a_1 ($e \times 10^{-3}$)	a_2 ($e \times 10^{-3}$)	e ($e \times 10^{-3}$)	total	a_1 ($e \times 10^{-3}$)	a_2 ($e \times 10^{-3}$)	e ($e \times 10^{-3}$)	total
$M-S_C$	84	0	131	215	63	0	113	176
$M-S_I$	102	0	118	220	89	0	99	188
$M-S_{II}$	72	6	147	225	61	5	119	185
$M-S_{III}$	46	24	143	213	42	20	124	186

clusters; (iii) the absolute values of Q_{S_C}, Q_M, and Q_{S_P} in **1** are definitely smaller than corresponding quantities in **2**. These data, coupled with those reported in Table 7, indicate that the metal−ligand bonding in **2** has a more ionic character than in **1**.[23]

A further point to be considered is the different nature of the lowest unoccupied levels ($56a_1 + 57a_1 + 81e$ MOs) in **1** and **2**. In the Cd derivative, the $56a_1$ and $57a_1$ MOs are significantly localized on the Cd 5s AOs, while in **1** the participation of the Zn 4s AOs to these levels is definitely lower. It is noteworthy that the $56a_1$ MO of **2** is the antibonding component of the low lying $52a_1$ level ($\Delta E(\mathbf{2}) = E_{56a_1} - E_{52a_1} = 5.19$ eV), while the antibonding partner of the same orbital in **1** is the higher lying $58a_1$ MO ($\Delta E(\mathbf{1}) = E_{58a_1} - E_{52a_1} = 6.59$ eV). A $\Delta E(\mathbf{1}) > \Delta E(\mathbf{2})$ is consistent with the higher covalency of the metal−ligand interaction in **1** than in **2**.

As a whole, the analysis of the electronic structure of title compounds allows us to assess that neither **1** nor **2** can be considered well-tailored molecular models of the extended metal chalcogenide semiconductors ZnS and CdS. As a matter of fact, the valence band top and the conduction band bottom of ZnS (CdS) are mainly localized on the S 3p and Zn 4s (Cd 5s) AOs, respectively.[25] Neither the HOMO nor the LUMO of **1** reproduce this feature,[26] while only the bottom of the CdS conduction band is satisfactorily modeled by the LUMO of **2**.

We now turn to assign the UV absorption spectrum of **1** by referring to ground-state results (see Figure 3 and Table 4). The lowest lying transitions of **1** should be mainly localized on the $[S-As(CH_3)_2-S]^-$ ligand, implying the transfer of an electron from the S $3p_\pi$-based AOs (the $a_2 + e + 2t_1 + t_2$ linear combinations of the S_P; see Table 4) to the As 4s-based levels ($a_1 + e + t_2$). Partial DOS displayed in Figure 5 indicate that the ΔE associated with these transitions is ∼4 eV, in excellent agreement with the threshold of the UV spectrum of **1** (310 nm).[27] The shoulder at 277 nm (∼4.5 eV) can be then reasonably assigned to the excitation of an electron from the S $3p_\sigma$ MOs (see Table 4) to the As 4s levels. Theoretical ΔE's, once again in good agreement with experiment, range between 4.5 and 4.9 eV, indicating that S $3p_\sigma \rightarrow$ As 4s transitions cover an energy range extending to the band at 248 nm (5.00 eV). Incidentally, under this band should also be hidden LMCT transitions mainly localized in the $Zn_4(\mu_4\text{-}S)$ core which involve the transfer of an electron from the 3p S_C-based orbitals (t_2) to the Zn 4s levels ($a_1 + t_2$). The ΔE between the $74e/53a_1$ (see Table 4) MOs and the $58a_1$ MO is 5.0 eV, while the ΔE between the $74e/53a_1$ levels and the $83e/59a_1$ orbitals is 5.39 eV.[28] These data indicate that LMCT transitions strongly contribute also to the intense band below 240 nm. Such a result is in our opinion particularly interesting for two reasons: (i) it perfectly matches data reported by Blasse *et al.*[7] for $Zn_4(\mu_4\text{-}S)^{6+}$ clusters encapsulated in a borate cage; (ii) it indicates that, even if **1** cannot be considered a good molecular model of the extended ZnS, its inner core mimics very well the $Zn_4(\mu_4\text{-}S)^{6+}$ clusters encapsulated into cuboocta-hedral cavities of $Zn_4S(BO_2)_6$.

The theoretical results we obtained for the Cd derivative (see Table 5) are very useful even in the absence of good-quality UV data for **2**. Actually, in agreement with data reported by Blasse *et al.*[7] for $Cd_4(\mu_4\text{-}S)^{6+}$ clusters encapsulated in an aluminate cage, they point out that LMCT transitions localized in the $Cd_4(\mu_4\text{-}S)$ core have ΔEs >4 eV. In detail, the weighted mean value of the ground state ΔE associated with the excitation of an electron from the 3p S_C-based AOs ($74e/53a_1$ MOs) to the Cd 5s AOs ($56a_1 + 57a_1/81e$ MOs) is 4.27 eV. This result seems to indicate that the assignment proposed by Herron *et al.*[12] for the sharp excitonic feature in the UV absorption spectrum of the thiophenolate-capped cluster $[Cd_{20}(\mu_4\text{-}S)(\mu_3\text{-}S)_{12}(\mu\text{-}SPh)_{18}(SPh)_4]^{8-}$ has to be considered with some care.

4. Conclusions

In this paper we have presented the results of the first theoretical/spectroscopic study of the electronic structure of two sulfide clusters characterized by the presence of a S atom tetrahedrally coordinate to four Zn/Cd ions placed at the center of a distorted tetrahedron of S atoms. Despite such a structural arrangement, neither the Zn derivative nor the Cd one can be considered molecular models of extended systems. Nevertheless, LMCT transitions localized in the $M_4(\mu_4\text{-}S)$ inner core of the title compounds perfectly reproduce both in nature and in energy the maximum absorption of $Zn_4(\mu_4\text{-}S)^{6+}$ and $Cd_4(\mu_4\text{-}S)^{6+}$ clusters encapsuled in borate and aluminate cages.

Acknowledgment. This work was partially supported by Progetto Finalizzato "Materiali Speciali per Tecnologie Avanzate II" of the CNR (Rome). We also thank Dr. F. Röminger, Organisches-Chemische Institüt, University of Heidelberg, for the X-ray data collection and Dr. P. Traldi of the CSRCC, CNR (Padova), for the ESI mass spectra. One of us (A.A.) acknowledges financial support from the Vigoni program.

Supporting Information Available: Tables listing detailed crystallographic data, atomic positional parameters, bond lengths, bond angles, and fully labeled figures for the four independent molecules of compounds **1**. This material is available free of charge via the Internet at http://pubs.acs.org.

IC980914A

(23) Both the first and the second ionization potentials of Cd (8.99 and 16.91 eV) are significantly lower than those of Zn (9.39 and 17.96 eV),[24] so that it is not particulaly surprising that the Cd−ligand interactions are more ionic than the Zn−ligand ones.

(24) *Handbook of Chemistry and Physics*, 64th ed.; CRC Press: Boca Raton, FL, 1984.

(25) Jørgensen, C. K. *Inorganic Complexes*; Academic Press: New York, 1963.

(26) At variance to S_C, quasi-tetrahedrally coordinated to four Zn (Cd) ions, the S_P atoms of the $S-As(CH_3)_2-S$ ligand cannot be considered as representative of sulfide ions in the extended ZnS (CdS).

(27) In the free $[S-As(CH_3)_2-S]^-$ ligand, the excitation of an electron from the S 3p nonbonding orbitals to the As 4s AO corresponds to a ΔE of 3.8 eV.

(28) The $58a_1$ MO (−1.54 eV) of **1** is the totally symmetric combination of the Zn 4s AOs, while the t_2 combination is accounted for by the $59a_1 + 83e$ MOs (−1.17 and −1.16 eV, respectively).